

## The effects of pyrolytic carbon interphase thickness on the properties of hot-pressed SiC<sub>f</sub>/SiC composites

Alfian Noviyanto and Dang-Hyok Yoon\*

School of Materials Science and Engineering, Yeungnam University, Gyeongsan 712-749, Korea

The effects of pyrolytic carbon interphase (PyC) thickness on the density, microstructure, and mechanical properties of continuous SiC fiber-reinforced SiC composites (SiC<sub>f</sub>/SiC) have been examined. Electrophoretic deposition combined with ultrasonication was performed to infiltrate a SiC-based matrix phase effectively into the fine voids of a Tyranno-SA SiC fabric preform, which was coated with PyC at thicknesses of 0, 200, 400, 600, and 800 nm. The density of the hot-pressed SiC<sub>f</sub>/SiC composites decreased with increasing PyC thickness because of the difficulty of matrix-phase infiltration into the fine voids of the preform. SiC<sub>f</sub>/SiC composites with PyC ≤ 400 nm showed a brittle fracture mode due to the strong fiber-matrix interface, in spite of their relatively high flexural strength. On the other hand, toughened SiC<sub>f</sub>/SiC composites could be achieved with PyC ≥ 600 nm because of the formation of a weak interface, in spite of their decreased flexural strength.

**Key words:** SiC<sub>f</sub>/SiC composites, Interphase, Mechanical properties, Fiber pullout.

### Introduction

Thanks to its excellent thermal, chemical and mechanical properties, a SiC-based ceramic has been considered as one of the most attractive materials for applications under severe conditions [1, 2]. However, the brittle nature of monolithic SiC ceramic is the main limitation on expanding its practical applications. Therefore, a fiber-reinforced composite structure has been suggested to enhance damage tolerance upon fracturing by deflecting the crack propagation path at the interface between the matrix and the fibers [3]. It is believed that the presence of a weak interface is very important for crack deflection in fiber-reinforced composite, including continuous SiC fiber-reinforced SiC composites (SiC<sub>f</sub>/SiC), where a pyrolytic carbon (PyC) coating has been generally used for this purpose [3].

Although SiC<sub>f</sub>/SiC was initially designed for aerospace and energy-related applications, it has been recently considered as a structural component for fusion and advanced fission reactors because of its low induced radioactivity and favorable resistance to neutron irradiation conditions [4, 5]. Among many SiC fibers introduced so far, Tyranno-SA fiber is known to be the most thermally robust without showing any strength degradation or compositional changes up to 2,200 °C in an inert atmosphere [6]. Because this fiber consists mainly of β-SiC crystals with a C/Si atomic ratio of 1.08, in addition, good

irradiation resistance can also be expected due to its highly crystalline structure and near stoichiometric composition [6].

A dense microstructure and damage-tolerance of SiC<sub>f</sub>/SiC are essential for practical applications in energy-related and nuclear reactor areas. However, the main current limitation on fabricating a SiC<sub>f</sub>/SiC composite is the lack of a suitable manufacturing technique. Most of the infiltration methods suggested so far, such as chemical vapor infiltration (CVI), polymer impregnation and pyrolysis (PIP), and reaction sintering (RS), resulted in a significant amount of residual porosity [7-10]. Recently, a new method has been introduced for dense SiC<sub>f</sub>/SiC composite fabrication using electrophoretic deposition (EPD) combined with ultrasonication, which has achieved an SiC<sub>f</sub>/SiC density of ≥ 99.5%, among the highest ever reported [11]. Even though this method was basically modified from the nano-infiltrated transient eutectoid (NITE) method which used the conventional dipping method for infiltration [12, 13], it was able to minimize the "surface sealing effect" using the periodic ultrasonic pulses during electrophoretic infiltration. However, all the SiC<sub>f</sub>/SiCs fabricated using 400 nm-thick PyC coated SiC fabric showed a brittle fracture behavior in spite of their high density [11].

With these backgrounds, the effect of PyC interphase coating thickness on Tyranno-SA SiC fiber on the microstructure and mechanical properties of SiC<sub>f</sub>/SiC has been examined in this study. The objective was to find the optimum PyC coating thickness to confer toughness as well as to understand the overall composite properties as a function of PyC thickness.

\*Corresponding author:  
Tel : +82-538102561  
Fax: +82-538104628  
E-mail: dhyoon@ynu.ac.kr

## Experimental

A mixture of nano-sized  $\beta$ -SiC (4620KE, NanoAmor Inc., USA) and 12 wt. %  $\text{Al}_2\text{O}_3$  and  $\text{Y}_2\text{O}_3$  sintering additive, at a weight ratio of 7.1:2.9, was used as the matrix phase. To make the additive particle size comparable to fine  $\beta$ -SiC powder ( $D_m = 52 \text{ nm}$ ) for homogeneous mixing, high-energy milling (MiniCer, Netzsch, Germany) of the additive was performed for 3 hours using 0.8 mm  $\text{ZrO}_2$  beads at 3,000 rpm, achieving a mean particle size of 192 nm. Two-dimensionally woven Tyranno-SA grade-3 fabrics (Ube Industries LTD., Japan), which had a  $0/90^\circ$  plain woven structure containing 1,600 filaments per yarn, were used as reinforcements after being punched into 5 cm-diameter discs. Images of the  $\beta$ -SiC particles, sintering additive, and fabric preform are shown in Fig. 1. The PyC layer was coated on SiC fabric through the decomposition of  $\text{CH}_4$  at 1,100 °C with a deposition pressure of 12 kPa for various times. As shown in Fig. 2, different PyC thicknesses of 200, 400, 600, and 800 nm on SiC fiber were obtained as a result.

The mixed powder of  $\beta$ -SiC and sintering additive was dispersed in ethanol, which had already dissolved 2 wt. % of polyvinyl butyral (PVB) resin with respect to the ethanol as a binder phase. This slurry for the matrix phase was further ball-milled for 36 hours using 6 mm SiC balls to ensure particle dispersion. EPD was performed using a dual electrode system for the SiC preform under an applied voltage of 10 V for 30 minutes with the application of ultrasound. Five types of SiC fibers, with PyC thicknesses of 0, 200, 400, 600, and 800 nm, were used as a preform. The distance between the SiC fabric and the stainless steel electrode was 20 mm. 10 W ultrasonic pulses with a one second cycle were applied only for the first 20 minutes to enhance the infiltration using a probe-type ultrasonicator (HD 2070, Bandelin, Germany). After drying the infiltrated fabrics at 70 °C for three

hours, 15 layers of fabrics having the same PyC thickness were stacked and laminated uni-axially under a pressure of 10 MPa at 80 °C. All samples underwent a binder burn-out process at 400 °C for two hours in air. Hot pressing was then carried out at 1,750 °C for 1 hour in an Ar atmosphere at a pressure of 20 MPa. More details of the experimental method, including the particle dispersion, slurry preparation, and EPD processes, can be found in previous reports by the authors [11, 14, 15].

The density of the composites was measured for five samples using the Archimedes method. The hot-pressed samples were cut into  $4 \times 2 \times 40 \text{ mm}^3$  pieces and polished for a three-point bending test (UTM AG-50E, Shimadzu, Japan), which was performed at a crosshead speed of 0.1 mm/minute and a span of 30 mm. The crystal structure of the hot-pressed composites was analyzed by X-ray diffraction (XRD: RINT 2200, Rigaku using  $\text{Cu K}\alpha$  line, 40 kV, and 40 mA). The sample morphology and phase distribution was determined by a scanning electron microscope (SEM; Hitachi S-4800) equipped with an energy-dispersive X-ray spectrometer (EDX: Horiba EX-250). Thermal etching of the polished specimen was carried out at 1500 °C for 1 hour to observe the grains by SEM.

## Results and Discussion

Fig. 3 shows the bulk density of hot-pressed SiC<sub>f</sub>/SiC composites as a function of PyC thickness along with their percentage densities, which were calculated by considering the theoretical density and volume content of each constituent phase. It was found that both densities decreased with increasing PyC thickness, for example, densities of 3.30 g/cm<sup>3</sup> (99.8%) and 2.92 g/cm<sup>3</sup> (96.0%) were observed for the composites having 0 and 800 nm PyC respectively. This decrease in bulk density with increasing PyC thickness can be explained by two reasons. One is the increased PyC volume

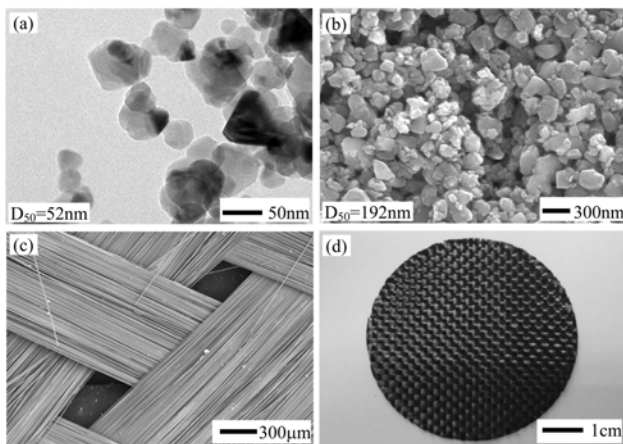


**Fig. 1.** Images of (a)  $\beta$ -SiC particles, (b)  $\text{Al}_2\text{O}_3$ - $\text{Y}_2\text{O}_3$  sintering additives after milling, (c)  $0/90^\circ$  woven Tyranno SA3 fabric and (d) SiC fabric disc used for infiltration.

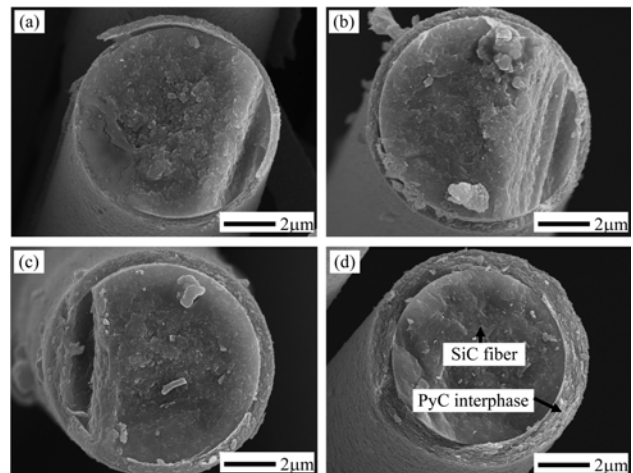


**Fig. 2.** SEM images of SiC fiber having various PyC interphase thicknesses: (a) 200, (b) 400, (c) 600 and (d) 800 nm.

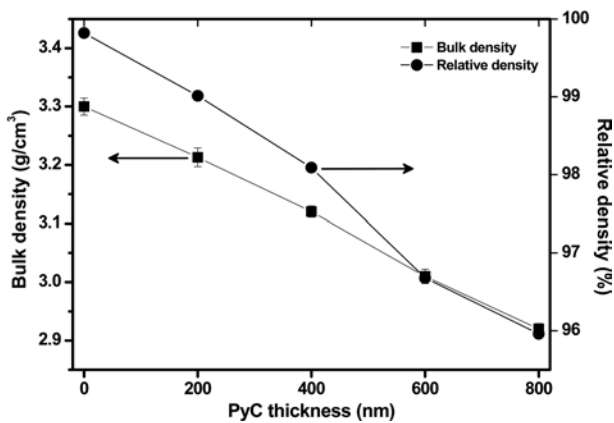


Fig. 3. Measured and calculated theoretical densities of hot-pressed  $\text{SiC}_f/\text{SiC}$  composites as a function of PyC thickness.

portion, which has a relatively lower density ( $\approx 2.0 \text{ g/cm}^3$ ) than SiC ( $= 3.21$  and  $3.10 \text{ g/cm}^3$  for powder and fiber respectively) and sintering additive ( $= 3.95, 5.03,$  and  $4.50 \text{ g/cm}^3$  for  $\text{Al}_2\text{O}_3, \text{Y}_2\text{O}_3,$  and  $\text{Y}_3\text{Al}_5\text{O}_{12}$  respectively). The other reason arises from the difficulty in infiltration of the matrix phase into the fine voids of the fabrics as the PyC thickness increases. Because the woven fabrics contain large inter-bundle

voids as well as fine intra-bundle voids between the fibers in a bundle, as shown in Fig. 1 (c), it can be hypothesized that infiltration into the fine voids becomes difficult because the size of the voids decreases as the PyC thickness increases.

Fig. 4 shows SEM images of the polished  $\text{SiC}_f/\text{SiC}$  composites which were fabricated with the fibers having different PyC thicknesses. When no PyC layer has been coated on the SiC fiber, as shown in Fig. 4 (a), the boundary between the fiber and the matrix phase cannot be distinguished due to complete consolidation, implying the monolith-like behavior of this  $\text{SiC}_f/\text{SiC}$  composite without a PyC interphase layer. The overall composite porosity seemed to increase with increasing PyC thickness due to the difficulty of matrix-phase infiltration, which is consistent with the density results shown in Fig. 3. In addition, it can also be observed that the border between the fiber and matrix phases, i.e., the PyC layer, gradually becomes dimmer and disappears at the boundary between the fiber- and matrix-rich regions. Because of the extra matrix phase surface-deposited onto the fabrics during the EPD process, all the  $\text{SiC}_f/\text{SiC}$  samples fabricated with this process had alternating layers of fiber-rich and matrix-rich regions, maintaining the overall fiber content in

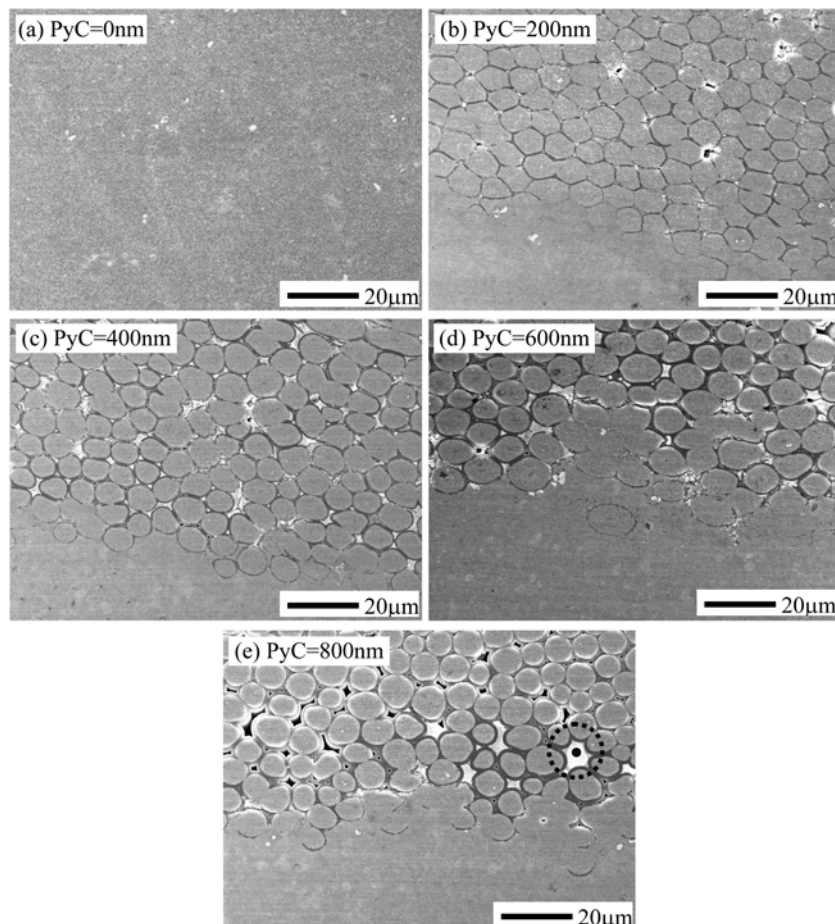
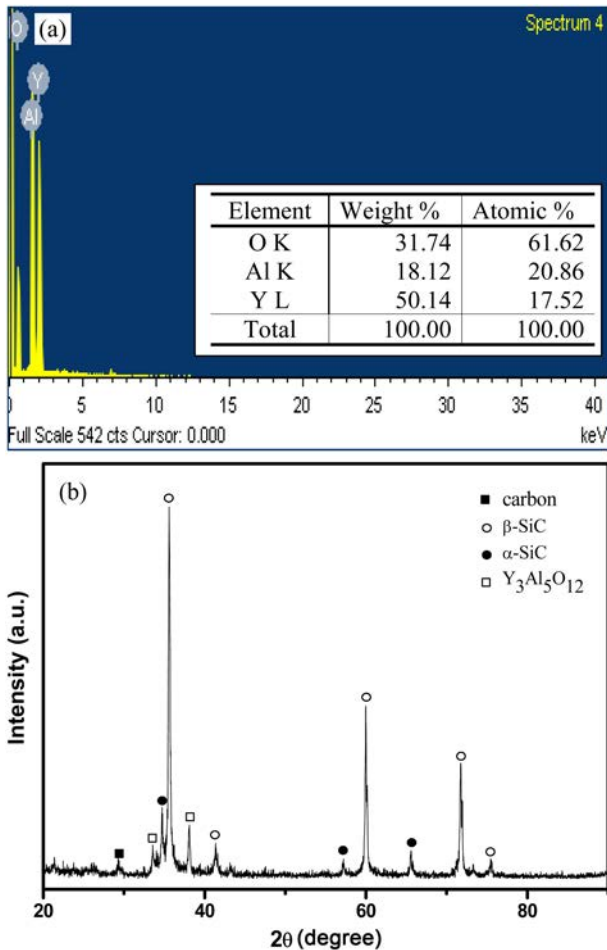
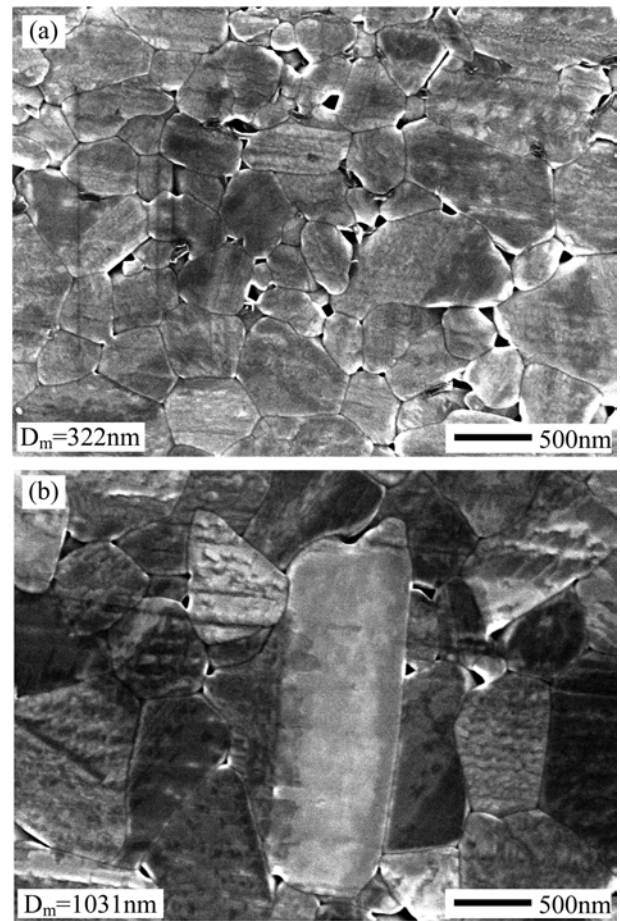


Fig. 4. SEM images of polished  $\text{SiC}_f/\text{SiC}$  composites having different PyC thicknesses.



**Fig. 5.** (a) EDX analysis results for the liquid phase (white-colored) marked in Fig. 4 (e), and (b) XRD pattern for the hot-pressed SiC<sub>f</sub>/SiC composite.

the composite between 45-50 vol.%. Because only the matrix phase contains the Al<sub>2</sub>O<sub>3</sub>-Y<sub>2</sub>O<sub>3</sub> additive, which forms a liquid phase during hot pressing, a possible reaction between PyC and the liquid phase that eliminates the PyC interphase can be expected [16]. One notable aspect of these images is the existence of a white phase in the inter-fiber voids, as marked by a dot in Fig. 4 (e), which was confirmed as a Y<sub>3</sub>Al<sub>5</sub>O<sub>12</sub> (yttrium aluminum garnet: YAG) phase according to further analyses. Figs. 5 (a) and 5 (b) represent the EDX results for the liquid phase (white-colored) and the XRD pattern for the composite respectively. The EDX data are quite close to the stoichiometric atomic ratio of Y<sub>3</sub>Al<sub>5</sub>O<sub>12</sub>, and the XRD pattern indicates clearly the existence of the YAG phase. Therefore, it can be hypothesized that liquid YAG was formed from Al<sub>2</sub>O<sub>3</sub> and Y<sub>2</sub>O<sub>3</sub> sintering additives during hot pressing and that it was preferentially located at the vacant voids between the fibers after acting as an aid to liquid-phase sintering. Even though the melting temperature of YAG is known to be ≥ 1900 °C under atmospheric conditions [17-19], it seemed to decrease to ≤ 1750 °C under this hot pressing condition.



**Fig. 6.** SEM images of the thermally-etched (a) fiber and (b) matrix of the SiC<sub>f</sub>/SiC composites, showing a larger grain size in the matrix than in the fiber region.

Fig. 6 compares the grain structures of the (a) fiber and (b) matrix regions, where the much larger grain size for the matrix region than that for the fiber can be observed. Because the Tyranno-SA3 fiber was produced by heat treatment of a polymeric precursor at 1800 °C, which is higher than the hot pressing temperature used in this study, the fiber showed uniform fine grains with a mean size of 322 nm. On the other hand, the matrix phase showed significant grain growth, up to a few μm, from the initial β-SiC particle size of 52 nm, which can be attributed to the effect of the additive for liquid-phase sintering. According to the XRD pattern shown in Fig. 5 (b), a certain amount of β-SiC had been transformed to α-SiC. This β- to α-SiC transformation is common at high temperatures and features a plate-like α-SiC grain structure, as shown in Fig. 6 (b) [20]. A small carbon peak originating from the PyC interphase can also be observed along with the YAG phase in the XRD pattern.

Fig. 7 presents the flexural strength-displacement behavior of the composites with different PyC thicknesses. The composites fabricated with the fiber having 0 and 800 nm-thick PyC showed flexural

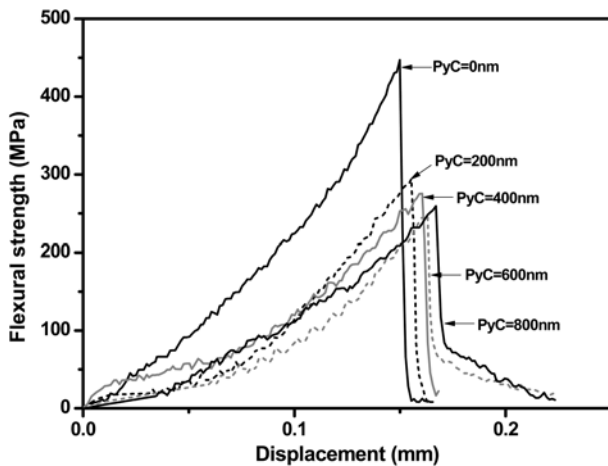


Fig. 7. Typical three-point bending test behavior of the  $\text{SiC}_f/\text{SiC}$  composites manufactured with different thicknesses of PyC layer.

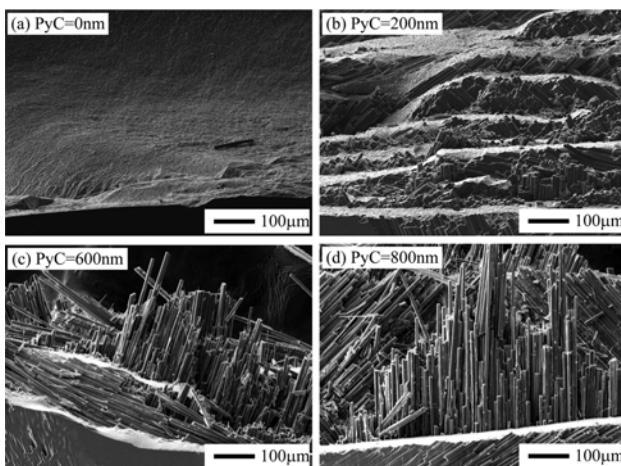


Fig. 8. SEM images of the fractured  $\text{SiC}_f/\text{SiC}$  surfaces after the three-point bending tests, showing the different degrees of fiber pullout with different PyC thickness.

strength of 447 and 259 MPa respectively; this strength decreased generally with increasing PyC thickness because of increasing porosity. The composites with  $\text{PyC} \leq 400$  nm showed an abrupt decrease in load after fracturing, which indicates the brittle nature of these composites. When the interface is too strong, brittle fracture can be expected because a crack passes through the interface as in a monolithic ceramic without any deflection of the crack propagation [3]. On the other hand, the  $\text{SiC}_f/\text{SiC}$  with  $\text{PyC} \geq 600$  nm showed some tail extension in their flexural strength-displacement behavior, as shown in Fig. 7. This prolonged tail indicates an increase in composite toughness because of the weak fiber-matrix interface, which was the main objective of fiber reinforcement. Based on these observations, it can be concluded that  $\text{PyC} \geq 600$  nm can form a weak fiber-matrix interface which may contribute to a toughness increase by crack deflection, while the  $\text{PyC} \leq 400$  nm cannot contribute to a toughness increase.

Fig. 8 shows SEM images of the fractured composite

surfaces after the three-point bending tests as a function of PyC thickness. The composite fabricated with the fibers without PyC coating showed a flat cleavage surface due to the strong consolidation between the fiber and matrix phases, as shown in Fig. 8 (a). On the other hand, the  $\text{SiC}_f/\text{SiC}$  fabricated with 600 and 800 nm PyC-coated SiC fiber showed a significant amount of fiber pullout, compared to the small amount of fiber pullout of the composite fabricated with 200 nm PyC. Because fiber pullout can be attributed to a weak fiber-matrix interface, the tail extension of the flexural strength-displacement curve shown in Fig. 7 for composites with  $\text{PyC} \geq 600$  nm is in agreement with this view of the fracture process. Based on these overall observations, the minimum PyC thickness which can confer toughness to the composite is 600 nm. Otherwise,  $\text{PyC} \leq 400$  nm may react with the liquid phase and form a strong fiber-matrix interface, which does not contribute to a toughness increase.

## Conclusions

This study has examined the effects of PyC interphase thickness on the properties of  $\text{SiC}_f/\text{SiC}$ . PyC thickness is believed to play an important role in conferring damage tolerance to the fiber-reinforced composite.  $\text{SiC}_f/\text{SiC}$ s with five different PyC thicknesses (0, 200, 400, 600 and 800 nm) have been successfully fabricated using electrophoretic infiltration combined with ultrasonication. The composite density after hot pressing decreased with increasing PyC thickness because of the increase in PyC volumetric content and the difficulty of infiltration of the matrix phase into the fine voids. In addition, the  $\text{Al}_2\text{O}_3\text{-Y}_2\text{O}_3$  sintering additive was found to form a liquid YAG ( $\text{Y}_3\text{Al}_5\text{O}_{12}$ ) phase during hot pressing, which promoted abnormal grain growth in the matrix phase. A possible reaction between the PyC interphase and this liquid phase, which could melt the PyC layer, was suggested. It was also observed that  $\text{PyC} \geq 600$  nm could form a weak fiber-matrix interface, resulting in a tail extension of the flexural strength-displacement curve, while  $\text{PyC} \leq 400$  nm showed an abrupt decrease in load after fracturing due to the strong fiber-matrix interface in spite of the relatively higher flexural strength. Based on these overall observations, PyC coatings  $\geq 600$  nm would have the optimum thickness for this process of electrophoretic infiltration combined with ultrasonication, which can provide toughness to  $\text{SiC}_f/\text{SiC}$  composites. However, further process optimization to obtain a high fracture toughness without sacrificing flexural strength is still needed.

## Acknowledgement

This research was supported by the Yeungnam University research grants in 2011.

## References

1. S.J. Dapkunas, *Am. Ceram. Soc. Bull.* 67 (1988) 388-391.
2. P. Baldus, M. Jansen, and D. Sporn, *Science* 285 (1999) 699-703.
3. R.J. Kerans, *Scripta Mater.* 32 (1995) 505-509.
4. B. Riccardi, L. Giancarli, A. Hasegawa, Y. Katoh, A. Kohyama, R.H. Jones, and L.L. Snead, *J. Nucl. Mater.* 329-333 (2004) 56-65.
5. Y. Hirohata, T. Jinushi, Y. Yamaguchi, M. Hashiba, T. Hino, Y. Katoh, and A. Kohyama, *Fus. Eng. Des.* 61-62 (2002) 699-704.
6. T. Ishikawa, Y. Kohtoku, K. Kumagawa, T. Yamamura, and T. Nagasawa, *Nature* 391 (1998) 773-775.
7. R. Yamada, T. Taguchi, and N. Igawa, *J. Nucl. Mater.* 283-287 (2000) 574-578.
8. K. Yoshida, M. Imai, and T. Yano, *Compos. Sci. Technol.* 61 (2001) 1323-1329.
9. T. Taguchi, N. Igawa, R. Yamada, and S. Jitsukawa, *J. Phys. Chem. Solids* 66 (2005) 576-580.
10. A. Ortona, A. Donato, G. Filacchioni, U. De Angelis, A. La Barbera, C.A. Nannetti, B. Riccardi, and J. Yeatman, *Fusion Eng. Des.* 51-52 (2000) 159-163.
11. G.Y. Gil, and D.H. Yoon, *J. Ceram. Proc. Res.* 12 (2011) 371-375.
12. S.P. Lee, H.K. Yoon, J.S. Park, Y. Katoh, A. Kohyama, D.H. Kim, and J. K. Lee, *Fus. Eng. Des.* 61-62 (2002) 717-722.
13. Y. Katoh, S.M. Dong, and A. Kohyama, *Fus. Eng. Des.* 61-62 (2002) 723-731.
14. J.H. Lee, P. Yonathan, D.H. Yoon, W.J. Kim, and J.Y. Park, *J. Ceram. Proc. Res.* 10 (2009) 301-307.
15. J.H. Lee, G.Y. Gil, and D.H. Yoon, *J. Kor. Ceram. Soc.* 46 [5] (2009) 447-452.
16. P. Yonathan, J.H. Lee, D.H. Yoon, W.J. Kim, and J.Y. Park, *Mater. Res. Bull.* 44 (2009) 2116-2122.
17. I. Warshaw, and R. Roy, *J. Am. Ceram. Soc.* 42 (1959) 434-438.
18. J.S. Abell, J.R. Harris, B. Cockayne, and B. Lent, *J. Mater. Sci.* 9 (1974) 527-537.
19. J.L. Caslavsky, and D.J. Viechnicki, *J. Mater. Sci.* 15 (1980) 1709-1718.
20. A.M. Kueck, and L.C. De Jonghe, *J. Eur. Ceram. Soc.* 28 (2008) 2259-2264.